



Original article

Synthesis of NiO nanoparticles and their evaluation for photodynamic therapy against HeLa cancer cells



Mohamad S. AlSalhi^{a,*}, Muhammad Hammad Aziz^{b,*}, M. Atif^{a,*}, Mahvish Fatima^c, Fozia Shaheen^d, Sandhanasamy Devanesan^a, W. Aslam Farooq^a

^a Department of Physics and Astronomy, College of Science, King Saud University, P O Box 2455, Riyadh 11451, Saudi Arabia

^b Department of Physics, COMSATS University Islamabad, Lahore, Pakistan

^c Department of Physics, University of Lahore, Lahore, Pakistan

^d Department of Physics, GC University Lahore, Lahore, Pakistan

ARTICLE INFO

Article history:

Received 24 October 2019

Revised 24 November 2019

Accepted 24 November 2019

Available online 2 December 2019

Keywords:

NiO NPs

Cytotoxicity

ROS

Cellular morphology

ABSTRACT

The worldwide increase in malignancy rates has caused an increase of research interest for compelling and safe materials used for cancer treatment. A standout amongst the most pervasive types of treatment for malignant growth is photodynamic therapy (PDT), which is viewed as an alternative to radiotherapy and chemotherapy. PDT utilizing metal-based nanoparticles (NPs) is anticipated to be a useful approach for the treatment of malignant tumors. In the present study, NiO NPs were synthesized via a chemical coprecipitation (CPT) technique and characterized using XRD, SEM, TEM, UV–Visible spectroscopy, and EDX spectroscopy. The particle size was measured to be in the range of 90–120 nm using different characterization techniques. UV–visible spectroscopy showed the maximum absorption band was 340 nm, which confirmed the formation of the NiO NPs. Subsequently, the cytotoxicity of the NiO NPs was studied using a HeLa cancer cell line at various concentrations (10–180 µg/mL). An MTT assay was carried out and the reactive oxygen species (ROS) were investigated to determine the cell killing effects and their relationship with the loss of cell viability upon treatment with NiO alone or in the presence of light. Our results show that a light dose of 100 J/cm² and NiO NPs concentration of 180 µg/mL exhibited an effective PDT outcome on cervical cancer cells. These key outcomes support the photokilling effect of NiO NPs as a potential treatment for cervical malignancy and their in-vivo application is inferred from their biocompatible properties.

© 2019 The Author(s). Published by Elsevier B.V. on behalf of King Saud University. This is an open access article under the CC BY-NC-ND license (<http://creativecommons.org/licenses/by-nc-nd/4.0/>).

1. Introduction

Nanotechnology can be used in nanomedicine to discover and develop new and improved drug delivery strategies for use in cancer therapy (Cory et al., 2008; Nie et al., 2007). In the field nanotechnology, particularly metallic nanoparticles interest is growing rapidly due to its various applications in pharmaceutical as well as in antifungal, antimicrobial and cytotoxicity effects. Synthesis process of nanoparticles is simple, eco-friendly, non-invasive and free from toxic chemicals (Kanagamani et al., 2019; AlSalhi et al., 2016; Balachandar et al., 2019). In regard metal oxide NPs, their small size and large surface area result in high chemical reactivity and physically intrinsic toxic properties (Hu et al., 2009; Devanesan et al., 2018; Boomi et al., 2019; AlSalhi et al., 2019). The immense potential toxicity of engineered NPs, including titanium dioxide, nickel oxide, and carbon nanotubes (CNTs), has resulted in significant research interest (Azhaguraja et al., 2017;

Abbreviations: CNTs, Carbon nanotubes; DMSO, Dimethyl sulphoxide; DNA, Deoxyribonucleic acid; NPs, Nanoparticles; PDT, Photodynamic therapy; XRD, X-ray diffraction; SEM, Scanning Electron Microscopy; TEM, Transmission Electron Microscope; EDX, Energy-dispersive X-ray.

* Corresponding authors at: Department of Physics and Astronomy, College of Science, King Saud University, P O Box 2455, Riyadh 11451, Saudi Arabia (M.S. AlSalhi, M. Atif). Department of Physics, COMSATS University Islamabad, Lahore, Pakistan (M.H. Aziz).

E-mail addresses: malsalhy@gmail.com, malsalhi@ksu.edu.sa (M.S. AlSalhi), hammadaziz@ciitlahore.edu.pk (M.H. Aziz).

Peer review under responsibility of King Saud University.



Production and hosting by Elsevier

<https://doi.org/10.1016/j.jksus.2019.11.033>

1018-3647/© 2019 The Author(s). Published by Elsevier B.V. on behalf of King Saud University.

This is an open access article under the CC BY-NC-ND license (<http://creativecommons.org/licenses/by-nc-nd/4.0/>).

Liu et al., 2007; Vamanu et al., 2008). To date, Ni nanomaterials have played an important role in the health and medical sector. The strong penetration capability of these nanomaterials allow them to be used in biological models, such as cellular organelles and cells, which mostly depends on their size (Chang et al., 2017; Sharma et al., 2012). During the preparation of metallic nanoparticles, laboratory environment safety for human being is very important because it may cause mild eyes, skin irritations and also affects the lungs and liver [Świdwiński Gajewska and Czerzak, 2014]. Therefore, it is necessary to study the properties of NiO NPs.

Free radical production of ROS is one of the primary mechanisms for the *in vivo* and *in vitro* toxicity of NPs. Oxidative stress may lead to a destructive inflammatory response causing damage to mitochondria/DNA in cancer cells by either apoptosis or necrosis (Amruta et al., 2013; Hancock et al., 2001; Kawanishi et al., 2012; Takehiko et al., 2017; Tuanwei and Lifeng, 2018). NiO NPs endow the production of ROS that cause DNA autophagy in rat lungs cancer cells (Sharma et al., 2012). Chronic ingestion research by Cameron et al., 2011 showed that exposure to Ni may cause neoplasms in rat and mice lungs. Ni ions provoke DNA damage in cells, which has been attributed to Ni ion migration toward the nuclear cell membrane (Tuanwei and Lifeng, 2018). Interestingly, nano-sized NiO could be used in the treatment of cancer due to its toxicity.

Cancer incidences are increasing globally leading to 9.6 million deaths in 2018. Recent studies reported the epidemiological variability in 20 different regions of world. These incidences are colorectal cancer (6.1%), prostate cancer (7.1%), stomach cancer (8.2%), liver cancer (8.2%) and breast cancer (11.6%) (Bray et al., 2018.). Synthesized nanoparticles were reported which was performed as excellent therapeutic agent to treat various types of cancers (Kanagamani et al., 2019, AlSalhi et al., 2016).

Cervical cancer is major cause of death among women, representing 23.3% of all deaths caused by malignancy (Basile et al., 2006). The potential role of chemically synthesized NPs in several clinical applications has led to an in-depth analysis of their *in vitro* toxicity in humans. Thus, another interdisciplinary field in nanoscience and biomedical science called nanotoxicology has been developed, which aims to investigate the promising toxicological applications of NPs (Hemant et al., 2017; Singh and Nalwa, 2007). Nanotechnology will have a good influence and impact on fundamental sciences, specifically in clinical applications such as PDT. The activation of NPs by a selective UV laser source causes necrosis in cancer tissue via its damaging effect on the cell, such as vascular obstruction or the release of singlet oxygen from the mitochondria to generate ROS (Atif et al., 2010, 2011; Fakhar-e-Alam et al., 2014; Fatima et al., 2014). Therefore, we have evaluated the anticancer effects of NiO NPs with and without PDT in the HeLa cancer cell line in this study.

2. Material and methods

2.1. Preparation of NiO NPs

NiO NPs were synthesized using a co-precipitation method. NiSO₄·6H₂O and Na₂CO₃ at a molar ratio of 0.003:0.03 were used as starting materials and were mixed in 200 mL of deionized water at room temperature using a magnetic stirrer. After 30 min, the Na₂CO₃ solution was added dropwise to the NiSO₄·6H₂O solution heated at 50 °C. The mixed solution was allowed to stir continuously until a light green precipitate was obtained. The solution was washed three times with acetone to separate the precipitate. The precipitate was filtered and dried in an oven at 105 °C for 24 h. The light green powder was then sintered at 500 °C for 2 h.

At this temperature, the water was completely removed and the NiO NPs were obtained as a black powder.

2.1.1. Cell culturing and exposure to NiO NPs

HeLa cancer cell line was cultured in T75 flasks and added with 10% Hanks salts supplemented with 2 mL of glutamine and 10 mL of fetal bovine serum (FBS). Cells were incubated at 37 °C for 24 h, furthermore cells were also sub-cultured one or twice per week. The cells were then collected with trypsin when grown to 75–85% confluence (Fakhar-e-Alam et al., 2014; Fatima et al., 2014). The HeLa cells were then cultured on a 96 well plate for 24 h prior to treatment with the NiO NPs. The NiO NPs were diluted and suspended in cell culture medium to achieve the suitable concentrations studied.

2.1.2. Measurement of the *in vitro* cellular cytotoxicity using an MTT assay

HeLa cells were seeded on a 96-well culture plate and incubated at 37 °C under a 5% CO₂ atmosphere with and without the NiO NPs in the concentration range from 10 to 180 µg/mL for 24 h. Each well was subjected to an MTT assay followed by AlSalhi et al., 2016.

2.1.3. Membrane integrity

The lactate dehydrogenase (LDH) leakage was used to determine the cell membrane integrity of the HeLa cells *in vitro* using a TOX7 assay kit. HeLa cells were exposed to various concentrations of the NiO NPs (0–180 µg/mL) for 24 h in a 96-well plate. Then, 100 µL of the LDH mixture was added to each well in the 96-well plate. A microplate reader at 510 nm was used to record the optical density.

2.1.4. Reactive oxygen species

Intracellular ROS generation was detected using CMH2DCFDA (Invitrogen Partnership, USA). CMH2DCFDA passes through the cell membrane and experiences demobilization by esterases to form non-fluorescent CMH2DCF, which reacts with oxygen species within the cell. Subsequently, the cells were treated with various concentrations of the NiO NPs at 37 °C for 12 h under a humidified 5% of CO₂ atmosphere.

2.1.5. Cell morphology

HeLa cancer cells were seeded a in six-well plate (1 × 10⁴ cells per well) and incubated with various concentrations of the NiO NPs (10–180 µg/mL). Inverted phase contrast microscopy was used to evaluate the cell morphology to identify any changes in the HeLa cells induced by the NiO NPs with and without PDT.

2.1.6. PDT of HeLa cells

For PDT, HeLa cancer cells were seeded in a 96-well plate (5 × 10³ cells/well) and incubated with various concentrations of the NiO NPs (10–180 µg/mL) at 37 °C. Then, the cells were irradiated with red light (660 nm, 100 J/cm²) (Atif et al., 2011).

2.2. Characterization

The NiO NPs were characterized using XRD, SEM, TEM, EDX and UV-Visible spectroscopy (Shimadzu, UV-2450). The morphology of the NiO NPs was observed using SEM (JEOL, JSM-6480) and TEM (JEM-1011, JEOL, Tokyo, Japan). The results obtained for the NiO NPs were interpreted using a Philips®/PanalyticalX'Pert-Pro. The particle size and equal distribution of the NiO NPs were evaluated using the Scherrer equation shown below:

$$D_{\beta} = 0.89\lambda/\beta\cos\theta$$

where λ is the wavelength of radiation and β is the full width half maximum (FWHM).

3. Results

The XRD pattern obtained for the NiO NPs exhibits sharp diffraction peaks at 37.5, 43.4, 62, and 75°, which can be indexed to the (1 1 1), (2 0 0), (2 2 0) and (3 1 1) planes, respectively, as shown in Fig. 1. The sharp peaks indicate that NiO was in the present sample. The crystallite size of the NiO NPs was calculated to be 40–45 nm using the Scherrer equation.

The morphology of the NiO NPs was investigated using SEM and TEM, as shown in Fig. 2. The average crystallite size lie in the range

of 50–60 nm. The SEM image in Fig. 2(a) shows the NiO NPs are cubic and spherical in shape, and were slightly agglomerated. The formation of cubic and spherical nanoparticles was also observed in the TEM image displayed in Fig. 2(b). The particle size was in the range of 50–55 nm, which was in agreement with the average crystallite size calculated from the XRD pattern. Elemental analysis was performed to evaluate the elemental composition of the NiO NPs using EDX spectroscopy. The EDX spectrum of the NiO NPs exhibits the peaks corresponding to Ni and O, as shown in Fig. 2(c).

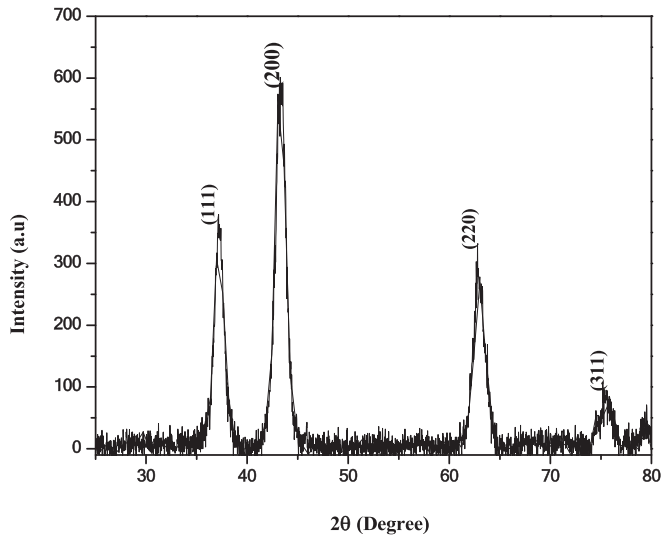


Fig. 1. XRD pattern obtained for the NiO NPs.

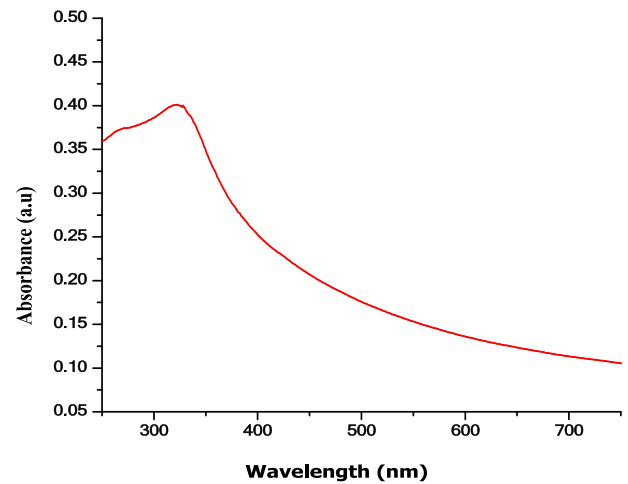


Fig. 3. UV-visible spectrum recorded for the NiO NPs.

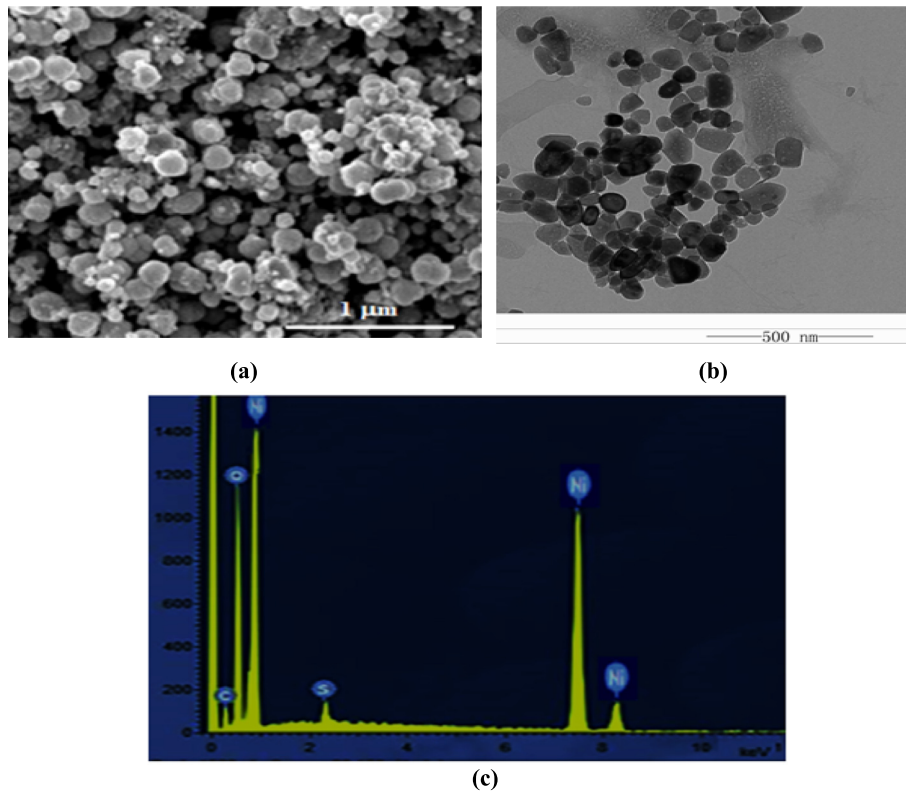


Fig. 2. (a) SEM, (b) TEM, and (c) EDX analysis of the NiO NPs.

Fig. 3 shows the UV–Visible spectrum of the NiO NPs, which has a maximum absorption band at 340 nm, which confirms the formation of the NiO NPs. This type of resonance is observed when the wavelength of the incident light surpasses the particle diameter. Furthermore, increasing the concentration of NiO, the mean absorbance of the NiO nanocomposite was increased to 0.5 a.u., as shown in Fig. 4. These experimental results demonstrated the dependence of the loss of cell viability and ROS, which revealed prominent malignant cell/tissue damage via cell necrosis/apoptosis.

We attempted to trace the maximum absorbance, optical density trend, and optimal dose using various concentrations (10, 30, 60, 90, 120, 150, and 180 $\mu\text{g}/\text{mL}$) of the NiO NPs with particle sizes in the range of 90–120 nm. The results after incubation for 24 and 48 h are shown in Fig. 5(a) and (b), respectively. The time taken for significant uptake of the NiO NPs solution (~48 h) was optimized.

The results demonstrate that the effect of the NiO NPs on the integrity of the cell membrane of HeLa cells occurred in a dose, time (24 h) dependence, manner and increased as the concentration of the NiO NPs increased, as shown in Fig. 6. A slight increase in the LDH activity was observed at a dose of 40–180 $\mu\text{g}/\text{mL}$ when compared to the control cells. In this study, we observed an excess amount of LDH leakage occurs in HeLa cancer cells upon increasing the concentration of the NiO NPs.

Fig. 7 shows that the liberation of ROS was directly proportional to the accumulation of NiO NPs in the biological cells. However, the exact mode of action, in which the NiO NPs generate ROS in the cells, is still under study. Fig. 7(a–d) show the fluorescence microscopy images of HeLa cancer cells displaying the generated intracellular ROS. It is perceived that green fluorescence illustrates the presence of intracellular ROS in the cells. Fig. 7(a) shows the control HeLa cells, while Fig. 7(b–d) show the HeLa cell treated with the NiO NPs at concentrations in the range of 40–180 $\mu\text{g}/\text{mL}$.

PDT methods for cancer are based on a few basic parameters, i.e., the optimal dose of NPs and appropriate wavelength of light, which lead to cell death. Therefore, optimization of the PDT parameters (nanoparticle concentration, threshold dose of light, and loss of cell viability dependency) was carried out, as shown in Fig. 8.

The experimental data shows the major difference between the absence and presence of light after exposing the HeLa cancer cells to the NiO NPs. Using different concentrations of the NiO NPs in the presence of light (100 J/cm^2), only 30% cells were alive. The cell

viability and ROS images obtained using fluorescence microscopy show that treatment with the NiO NPs alone and the morphological variations observed under PDT using blue light at a wavelength of 430 nm (100 J/cm^2) in the presence of the NiO NPs were consistent with this excellent performance (Fig. 9(a) and (b), respectively).

4. Discussion

Ni NPs provide significant effects in biomedicine, in particular their toxicity in humans, and their number of applications have increased rapidly. Earlier studies have shown the cytotoxic effects of Ni NPs in various tissues and cells (Usman et al., 2012; Zhao et al., 2009). To evaluate their cytotoxicity, a systematic study was performed to analyze the deadlines of NiO NPs toward the HeLa cells.

The possible toxic effects of NiO NPs were evaluated in a HeLa cancer cell line model. The cytotoxic effects of any drug are not significant in the absence of a nanocarrier, such as ZnO (Ada et al., 2010; Fakhar-e-Alam et al., 2014). In our recent study, metal oxide NPs ($\alpha\text{-Fe}_2\text{O}_3$ and SiO_2) exhibit cytotoxicity via cellular apoptosis in an in vitro RD cell model, which is time and dose dependent (Fakhar-e-Alam et al., 2014; Fatima et al., 2014). In another study, the in vitro cytotoxicity of CuO NPs toward HepG2 cells was explored (Siddiqui et al., 2013). In the present study, the cytotoxic effects of NiO NPs were explored using HeLa cancer cells as an experimental model. The NiO NPs were used to pacify the possibility of cell death. Horie et al. (2011), a significant reduction was attained at a NiO NPs concentration of 350 $\mu\text{g}/\text{mL}$ after 2, 6, 12 and 16 h of incubation, which decreased the cell viability up to 71, 53, 42, and 41% respectively. After 24 h, A549 cells exposed to NiO NPs show typical dose-dependent toxicity (~40% cell viability) (Siddiqui et al., 2012). Cytotoxicity in HEP-2 and MCF-7 cells occurs when exposed to different concentrations of NiO NPs for 24 h (Leist and Jaattela, 2001). In our study, NiO NPs were used as an anticancer agent and their in-vitro cytotoxicity evaluated in cervical cancer cells using an MTT assay. After measuring the optimal dose (~180 $\mu\text{g}/\text{mL}$) for the significant uptake of the NPs, as shown in Fig. 4, the toxic effects of the NiO NPs were evaluated in the HeLa cancer cell line. Fig. 5 shows that the percentage loss of cellular viability in the presence of the NiO NPs reached 62 and 48% after 24 and 48 h, respectively, which displayed a dose dependent reduction in cell viability. A clear relationship between

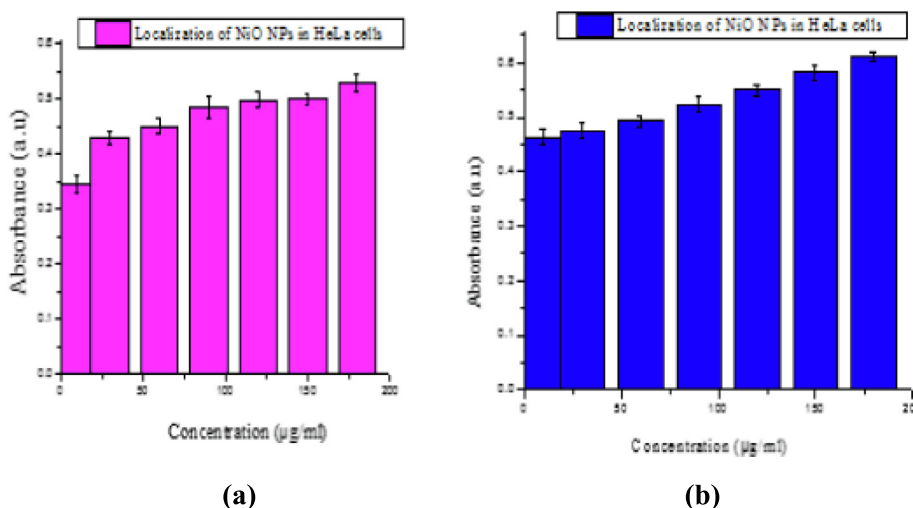
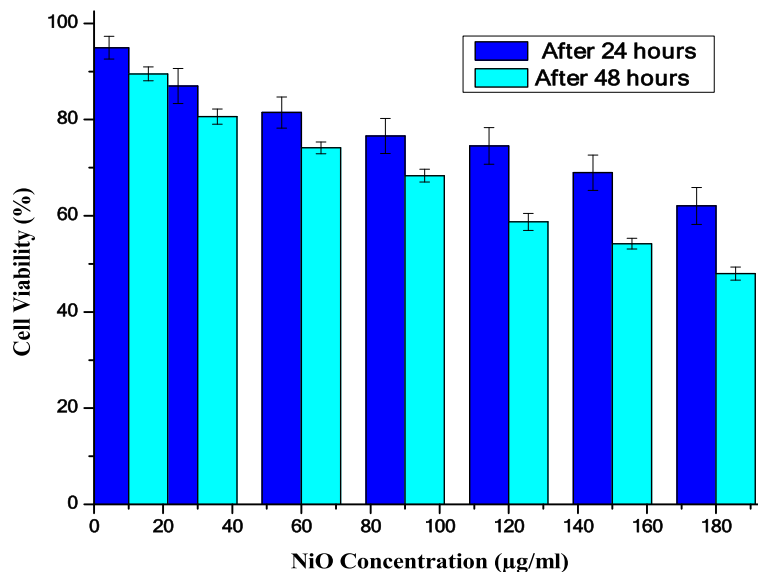


Fig. 4. Absorbance versus concentration of NiO NPs after incubation for (a) 24 and (b) 48 h.



(a)

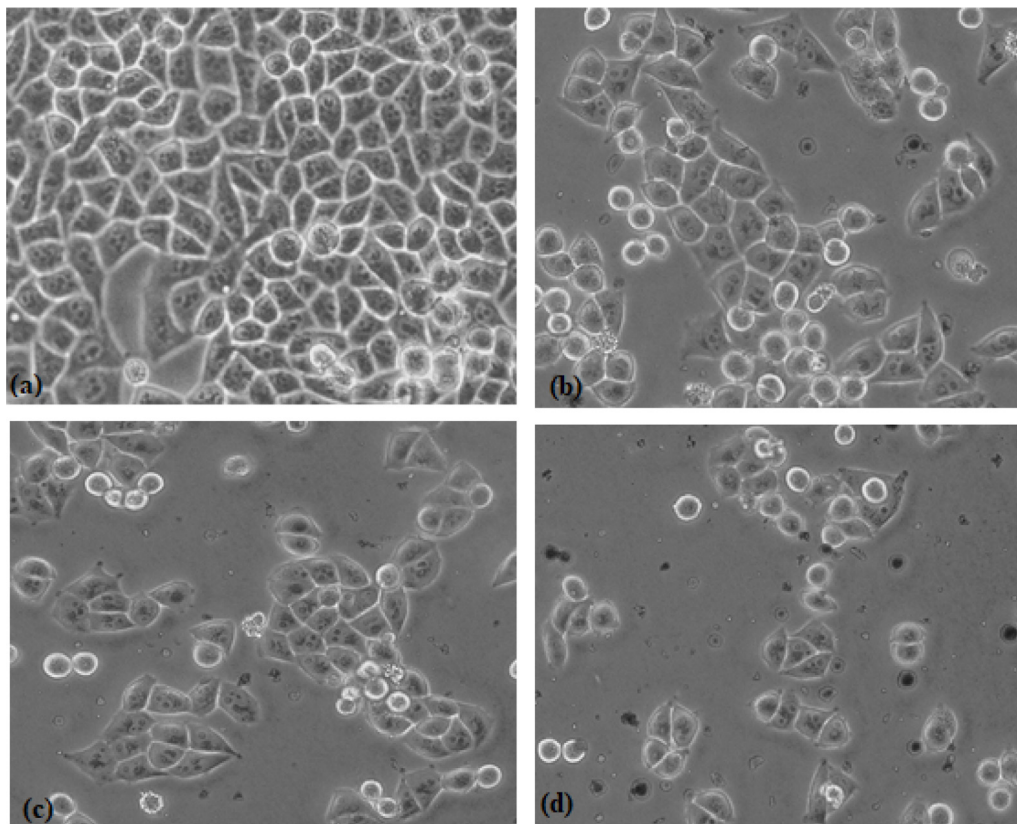


Fig. 5. (a) Loss of cell viability (%) in HeLa cells treated with NiO NPs after 24 and 48 h, respectively. The treated groups demonstrate statistically significant variances from the control group, as confirmed by the Student's *t*-test ($P < 0.05$). (b) The cellular destruction of HeLa cells by NiO NPs.

the cellular uptake and absorbance increases was observed, as shown in Fig. 4, in which the loss of cell viability loss increases gradually with an increase in the absorbance. The optimal concentration was selected to be 180 µg/mL because any further increase did not show any significant absorbance. In addition, at a NiO NPs concentration of 180 µg/mL, the cell viability increased to 48%, which is the unique feature of this experiment. Nevertheless,

previous data has given strong evidence that NiO NPs fulfil two basic criteria as an effective chemotherapeutic agent, i.e. tumor specificity and minimal toxicity to normal cells. In addition, the aforementioned results agreed with the previously published data, namely, the loss of cell viability is dose/concentration dependent (Horie et al. 2011). It is obvious from the given plot that a significant uptake of NPs was observed in the HeLa

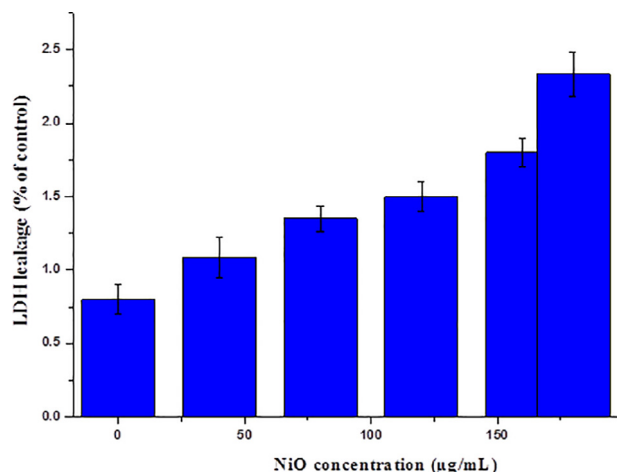


Fig. 6. LDH release (%) in HeLa cells following incubation with the NiO NPs for 24 h. The treated groups present statistically significant differences from the control group, as confirmed by the Student's *t*-test ($P < 0.05$).

cancer cell line. Cellular destruction in the HeLa cell line observed using inverted phase contrast microscopy revealed the morphological variation induced by the NiO NPs at different doses (Fig. 5(b)).

Apoptosis occurs due to cell membrane damage and the root cause of this phenomena was the release of LDH, a soluble cytosolic enzyme, into the extracellular medium. LDH is generally known as an indicator of lytic cell death (Leist and Jaattela, 2001). Due to the damage to the lysosomal membrane, which produces lysosomal membranes within the intercellular site, it may affect neighboring cells and trigger cell death via apoptosis. LDH leakage from particular cells is evidence for both the penetration of NPs into the cells and cell membrane damage (Aziz et al., 2016; Hussain et al., 2005).

The production of ROS and the loss of cell viability show the excellent killing effects of the NiO NPs in HeLa cells. These indicate that the NiO NPs interact with the tissue fluorophores to produce ROS, which leads to cell death and is in accordance with that previously reported (Aziz et al., 2016; Leist and Jaattela, 2001; Shukla et al., 2011; Xia et al., 2008; Atif et al., 2016). It was observed that the NiO NPs were capable of producing excessive oxidative stress in the targeted malignant cells. Oxidative stress can be involved in the cell killing process via damaging building block materials such proteins, DNA, and lipids, which is the precursor for several diseases. Oxidative stress increases the levels of ROS and hydrogen peroxide and the amount of catalase is decreased in damaged cells (Leist and Jaattela, 2001; Shukla et al., 2011; Xia et al., 2008). In short, when oxidative stress exceeds the antioxidant ability of

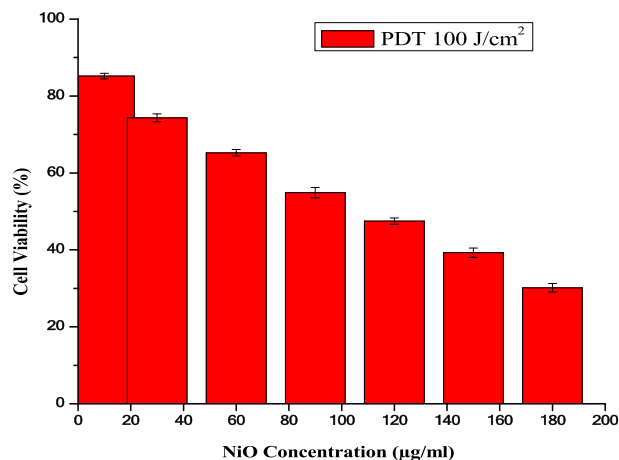


Fig. 8. The cell viability of HeLa cells treated with NiO NPs using PDT (100 J/cm²).

the cell, oxidative damage to critical biomolecules occurs, leading to cell death. ROS accretion is one of the key mechanisms in the programmed cell death process (Atif et al., 2010; Aziz et al., 2016). According to the above results, it is clear that low level lasers can affect the cellular permeability and mitochondria membrane potential. Therefore, cellular penetration of the NiO NPs is increased in the presence of light irradiation and the anticancer effect is increased due to their cellular uptake (Atif et al., 2019; Aziz et al., 2016).

5. Conclusion

In this work, NiO nanoparticles were synthesized using a co-precipitation method. The crystallography, morphology, and composition of the NiO NPs were confirmed by XRD, SEM and EDX spectroscopy, respectively. The particle size was confirmed to be in the range of 90–120 nm. The NiO NPs exhibit a major loss in cytotoxicity with enhanced bioavailability, including a loss of cell viability, localization of the NPs released in the given biological model and cell apoptosis. The results show that the cytotoxicity of NiO NPs toward HeLa cancer cells was dose-dependent via cell apoptosis. A NiO NPs concentration of 180 µg/mL shows a good response for cancer treatment. The current study concludes that NiO nanoparticles under appropriate light exposure (100 J/cm²) not only arrest the cell cycle, but also prevent HeLa cell proliferation by inducing oxidative stress through the liberation of ROS. This investigation may help advance research for prolonged drug exposure, which will be useful for biological applications e.g., cancer treatment, drug delivery, etc.

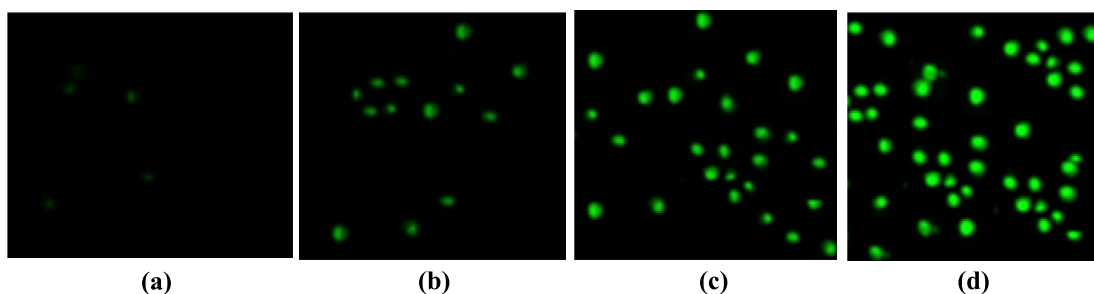


Fig. 7. ROS formation by H2DCFDA staining observed using fluorescence microscopy: (a) Control HeLa cells and HeLa cells in the presence of (b) 40 (c) 80, and (d) 160 µg/mL of NiO NPs.

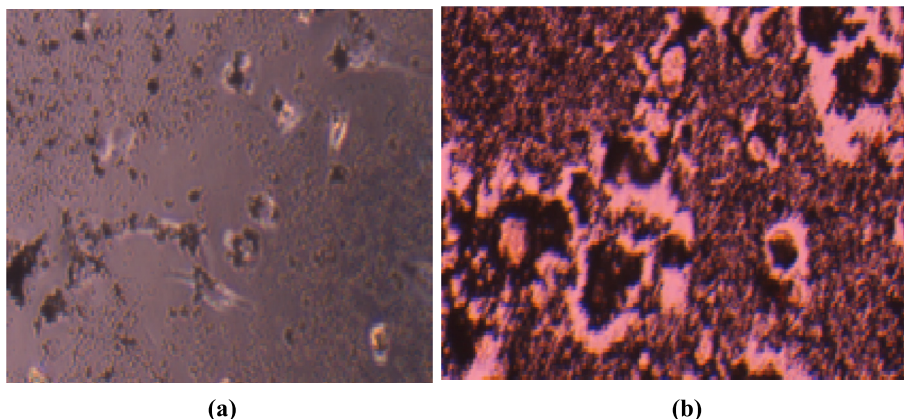


Fig. 9. The morphological changes in HeLa cells treated with (a) 40 and (b) 180 $\mu\text{g}/\text{mL}$ of NiO NPs in the presence of light exposure (100 J/cm^2).

Declaration of Competing Interest

The authors declare that they have no known competing financial interests or personal relationships that could have appeared to influence the work reported in this paper.

Acknowledgements

The authors are grateful to the Researchers Supporting Project Number (RSP-2019/68), King Saud University, Riyadh, Saudi Arabia.

References

- Ada, K., Turk, M., Oguztuzun, S., Kilic, M., Demirel, M., Nisa, T., Ertin, E., Latif, O., 2010. Cytotoxicity and apoptotic effects of nickel oxide nanoparticles in cultured HeLa cells. *Folia Histochem. Cytobiol.* 48, 524–529.
- AlSalhi, M.S., Devanesan, Alfuraydi, A.A., Vishnubalaji, R., Munusamy, M.A., Murugan, K., Nicoletti, M., Benelli, G., 2016. Green synthesis of silver nanoparticles using *Pimpinella anisum* seeds: antimicrobial activity and cytotoxicity on human neonatal skin stromal cells and colon cancer cells. *Int. J. Nanomed.*, 2016, 11, 4439.
- AlSalhi, M.S., Elangovan, K., Ranjitsingh, A.J.A., Murali, P., Devanesan, S., 2019. Synthesis of silver nanoparticles using plant derived 4-N-methyl benzoic acid and evaluation of antimicrobial, antioxidant and antitumor activity. *Saudi J. Biol. Sci.* 26, 970–978.
- Atif, M., Fakhar-e-Alam, M., Firdous, S., Zaidi, S.S.Z., Suleman, R., Ikram, M., 2010. Study of the efficacy of 5-ALA mediated photodynamic therapy on human rhabdomyosarcoma cell line (RD). *Laser Phys. Lett.* 7, 757–764.
- Atif, M., Fakhar-e-Alam, M., Sabino, L.G., Ikram, M., Araujo, M.T., Kurachi, C., Bagnato, V.S., AlSalhi, M.S., 2011. Analysis of the combined effect of lasers of different wavelengths for PDT outcome using 600, 630, and 660 nm. *Laser Phys. Lett.* 8, 386–392.
- Atif, M., Iqbal, Seemab, Fakhar-e-Alam, Muhammad, Ismail, Muhammad, Mansoor, Qaisar, Mughal, Lubna, Hammad Aziz, Muhammad, Hanif Atif, Aslam Farooq, W., Manganese doped cerium oxide nanocomposite induced Photodynamic therapy in MCF-7 cancer cells and antibacterial activity, *Biomed. Res. Int.*, 2019, 2019, Article ID 7156828.
- Atif, M., Fakhar-e-Alam, Muhammad, Abbas, Najeeb, A. Siddiqui, Maqsood, A. Ansari, Anees, A. Al-Khedhairi, Abdulaziz, M. Wang, Zhiming., In-vitro cytotoxicity of luminescent functionalized mesoporous $\text{SiO}_2@(\text{Eu}(\text{OH})_3)$ core-shell microspheres in MCF-7, *J. Nanomater.*, 2016, 2016, Article ID 7691861.
- Azhaguraja, R., AlSalhi, M.S., Devanesan, S., 2017. Microwave-assisted synthesis of nickel oxide nanoparticles using coriandrum sativum leaf extract and their structural-magnetic catalytic properties. *Materials* 10, 460–472.
- Aziz, M.H., Fakhar-E-alam, M., Fatima, M., Shaheen, F., Iqbal, S., Atif, M., Talha, M., Ali, S.M., Afzal, M., Majid, M., Al-Harbi, T.S., Zhiming, W.M., AlSalhi, M.S., Alahmed, Z.A., 2016. Photodynamic effect of Ni nanotubes on a HeLa cell line. *PLoS ONE* 11, e0150295.
- Balachandar, R., Gurumoorthy, P., Karmegam, N., Barabadi, H., Subbaiya, R., Anand, K., Boomi, P., Saravanan, M., 2019. Plant-mediated synthesis, characterization and bactericidal potential of emerging silver nanoparticles using stem extract of *Phyllanthus pinnatus*: a recent advance in phytonanotechnology. *J. Clust. Sci.* 30, 1481–1488.
- Basile, S., Angioli, S., Mancini, N., 2006. Gynecological cancers in developing countries: The challenge of chemotherapy in low-resources setting. *Int. J. Gynecol. Cancer.* 16, 1491–1497.
- Cameron, K.S., Buchner, V., Tchounwou, P.B., 2011. Exploring the molecular mechanisms of nickel-induced genotoxicity and carcinogenicity: a literature review. *Rev. Environ. Health.* 26, 81–92.
- Boomi, P., Poorani, G.P., Palanisamy, S., Selvam, S., Ramanathan, G., Ravikumar, S., Barabadi, H., Prabu, H.G., Jeyakanthan, J., Saravanan, M., 2019. Evaluation of antibacterial and anticancer potential of polyaniline-bimetal nanocomposites synthesized from chemical reduction method. *J. Clust. Sci.* 30, 715–726.
- Bray, F., Ferlay, J., Soerjomataram, I., Siegel, R.L., Torre, L.A., Jemal, A., 2018. Global cancer statistics 2018: GLOBOCAN estimates of incidence and mortality worldwide for 36 cancers in 185 countries. *CA Cancer J. Clin.* 68, 394–424.
- Chang, X.H., Zhu, A., Liu, F.F., Zou, L.Y., Su, L., Liu, S.K., Zhou, H.H., Sun, Y.Y., Han, A.J., Sun, Y.F., Li, S., Li, J., Sun, Y.B., 2017. Nickel oxide nanoparticles induced pulmonary fibrosis via TGF- β 1 activation in rats. *Hum. Exp. Toxicol.* 36, 802–812.
- Cory, H., Janet, L., Alex, P., Isaac, C., Andrew, C., Kevin, K., Denise, W., 2008. Preferential killing of cancer cells and activated human T cells using ZnO nanoparticles. *Nanotechnology* 19, 295103.
- Devanesan, S., AlSalhi, M.S., Balaji, R.V., Ranjitsingh, A.J.A., Ahamed, A., Alfuraydi, A. A., AlQahtani, F.Y., Aleanizy, F.S., Othman, A.H., 2018. Antimicrobial and cytotoxicity effects of synthesized silver nanoparticles from *Punica granatum* peel extract. *Nanoscale Res. Lett.* 13, 315.
- Fakhar-e-Alam, M., Rahim, S., Atif, M., Hammad, A.M., Imran, M.M., Zaidi, S.S., Suleman, R., Majid, A., 2014. ZnO nanoparticles as drug delivery agent for photodynamic therapy. *Laser Phys. Lett.* 11, 025601.
- Fatima, M., Fakhr-E-Alam, M., Atif, M., Zaidi, S.S., Suleman, R., Shakoore, M.N., Afzal, M., Waseem, M., Aziz, M.H., 2014. Apoptotic effect of $\alpha\text{-Fe}_2\text{O}_3$ and SiO_2 nanoparticles in human rhabdomyosarcoma cell line. *Laser Phys.* 24, 125602.
- Hancock, J.T., Desikan, R., Neill, S.J., 2001. Role of reactive oxygen species in cell signaling pathways. *Biochem. Soc. Trans.* 29, 345–350.
- Hemant, P.B., Chandrashekar, D.P., Rahul, K.S., Sunil, H.K., Bhavana, V.M., Giovanni, B., Satish, V.P., 2017. Mechanistic approach for fabrication of gold nanoparticles by *Nitzschia* diatom and their antibacterial activity. *Bioprocess Biosyst. Eng.* 40, 1437–1446.
- Horie, M., Fukui, H., Nishio, K., Endoh, S., Kato, H., Fujita, K., Miyauchi, A., Nakamura, A., Shichiri, M., Ishida, N., Kinugasa, S., Morimoto, Y., Niki, E., Yoshida, Y., Iwahashi, H., 2011. Evaluation of acute oxidative stress induced by NiO nanoparticles in vivo and in vitro. *J. Occup. Health.* 53, 64–74.
- Hu, X., Cook, S., Wang, P., Hwang, H.M., 2009. In vitro evaluation of cytotoxicity of engineered metal oxide nanoparticles. *Sci. Total Environ.* 407, 3070–3072.
- Hussain, S.M., Hess, K.L., Gearhart, J.M., Geiss, K.T., Schlager, J.J., 2005. In vitro toxicity of nanoparticles in BRL 3A rat liver cells. *Toxicol. In Vitro* 19, 975–983.
- Kanagamani, K., Muthukrishnan, P., Shankar, K., Kathiresan, A., Barabadi, H., Saravanan, M., 2019. Antimicrobial, cytotoxicity and photocatalytic degradation of norfloxacin using *Klebsiella grandiflora* mediated silver nanoparticles. *J. Clust. Sci.* 30, 1415–1424.
- Kawanishi, S., Oikawa, S., Inoue, S., Nishino, K., 2012. Distinct mechanisms of oxidative DNA damage induced by carcinogenic nickel subsulfide and nickel oxides. *Environ. Health Perspect.* 110, 789–791.
- Liu, X., Gurel, V., Morris, D., Murray, D., Zhitkovich, W.A., Kane, A.B., Hurt, R.H., 2007. Bioavailability of nickel in single-wall carbon nanotubes. *Adv. Mater.* 19, 2790–2796.
- Leist, M., Jaattela, M., 2001. Four deaths and a funeral: from caspases to alternative mechanisms. *Nat. Rev. Mol. Cell Biol.* 2, 589–598.
- Nie, S., Xing, Y., Kim, G.J., Simons, J.W., 2007. Nanotechnology applications in cancer. *Annu. Rev. Biomed. Eng.* 9, 257–288.
- Sharma, V., Anderson, D., Dhawan, A., 2012. Zinc oxide nanoparticles induce oxidative DNA damage and ROS-triggered mitochondria mediated apoptosis in human liver cells (HepG2). *Apoptosis* 17, 852–870.
- Shukla, R.K., Sharma, V., Pandey, A.K., Singh, S., Sultana, S., Dhawan, A., 2011. ROS-mediated genotoxicity induced by titanium dioxide nanoparticles in human epidermal cells. *Toxicol. In Vitro* 25, 231–241.

- Siddiqui, M.A., Ahamed, M., Ahmad, J., Majeed Khan, M.A., Musarrat, J., Al-Khedhairy, A.A., Alrokayan, A.A., 2012. Nickel oxide nanoparticles induce cytotoxicity, oxidative stress and apoptosis in cultured human cells that is abrogated by the dietary antioxidant curcumin. *Food Chem. Toxicol.* 50, 641–647.
- Siddiqui, M.A., Alhadlaq, H.A., Ahmad, J., Al-Khedhairy, A.A., Musarrat, J., Ahamed, M., 2013. Copper oxide nanoparticles induced mitochondria mediated apoptosis in human hepatocarcinoma cells. *PLOS ONE* 8, e69534.
- Singh, S., Nalwa, H.S., 2007. Nanotechnology and health safety-toxicity and risk assessments of nanostructured materials on human health. *J. Nanosci. Nanotechnol.* 7, 3048–3072.
- Świdwińska-Gajewska, A.M., Czerczak, S., 2014. Nanosilver – harmful effects of biological activity. *Med. Pr.* 65, 831–845.
- Takehiko, N., Kenichi, M., Naomi, T.H., 2017. Transgenic rat models for mutagenesis and carcinogenesis. *Gene Environ.* 39, 11.
- Tuanwei, L., Lifeng, Y., 2018. Functional polymer nanocarriers for photodynamic therapy. *Pharmaceuticals* 11, 133.
- Vamanu, C., Mihaela, R.C., Paul, J.H., Steinar, S., Stein, A.L., Nils, R.G., 2008. Induction of cell death by TiO₂ nanoparticles: studies on a human monoblastoid cell line. *Toxicol. In Vitro* 22, 1689–1696.
- Xia, T., Kovoichich, M., Liang, M., Mädler, L., Gilbert, B., Shi, H., Yeh, J.I., Zink, J.I., Nel, A.E., 2008. Comparison of the mechanism of toxicity of zinc oxide and cerium oxide nanoparticles based on dissolution and oxidative stress properties. *ACS Nano* 2, 2121–2134.
- Zhao, J., Bowman, L., Zhang, X., Shi, X., Jiang, B., Castranova, V., Ding, M., 2009. Metallic nickel nano- and fine particles induce JB6 cell apoptosis through a caspase-8/1F mediated cytochrome c-independent pathway. *J. Nanobiotechnol.* 7, 2.